ADVANCES IN ATMOSPHERIC SCIENCES, VOL. 32, MARCH 2015, 424–438

Processes Leading to Second-Year Cooling of the 2010–12 La Niña Event, Diagnosed Using GODAS

FENG Licheng*[1], ZHANG Rong-Hua[2,3], WANG Zhanggui[1], and CHEN Xingrong[1]

[1]*National Marine Environmental Forecasting Center, State Oceanic Administration, Beijing* 100081
[2]*Key Laboratory of Ocean Circulation and Waves, Institute of Oceanology, Chinese Academy of Sciences, Qingdao* 266071
[3]*Earth System Science Interdisciplinary Center (ESSIC), University of Maryland, College Park, Maryland, USA,* 20740

(Received 7 February 2014; revised 12 July 2014; accepted 22 July 2014)

ABSTRACT

Isopycnal analyses were performed on the Global Ocean Data Assimilation System (GODAS) to determine the oceanic processes leading to so-called second-year cooling of the La Niña event. In 2010–12, a horseshoe-like pattern was seen, connecting negative temperature anomalies off and on the Equator, with a dominant influence from the South Pacific. During the 2010 La Niña event, warm waters piled up at subsurface depths in the western tropical Pacific. Beginning in early 2011, these warm subsurface anomalies propagated along the Equator toward the eastern basin, acting to reverse the sign of sea surface temperature (SST) anomalies (SSTAs) there and initiate a warm SSTA. However, throughout early 2011, pronounced negative anomalies persisted off the Equator in the subsurface depths of the South Pacific. As isopycnal surfaces outcropped in the central equatorial Pacific, negative anomalies from the subsurface spread upward along with mean circulation pathways, naturally initializing a cold SSTA. In the summer, a cold SSTA reappeared in the central basin, which subsequently strengthened due to the off-equatorial effects mostly in the South Pacific. These SSTAs acted to initiate local coupled air–sea interactions, generating atmospheric–oceanic anomalies that developed and evolved with the second-year cooling in the fall of 2011. However, the cooling tendency in mid-2012 did not develop into another La Niña event, since the cold anomalies in the South Pacific were not strong enough. An analysis of the 2007–09 La Niña event revealed similar processes to the 2010–12 La Niña event.

Key words: La Niña, second-year cooling, off-equatorial effects, isopycnal analyses, circulation pathways, GODAS

Citation: Feng, L. C., R.-H. Zhang, Z. G. Wang, and X. R. Chen, 2015: Processes leading to the second-year cooling of the 2010–12 La Niña event, diagnosed using GODAS. *Adv. Atmos. Sci.*, **32**(3), 424–438, doi: 10.1007/s00376-014-4012-8.

1. Introduction

The El Niño–Southern Oscillation (ENSO) is the leading mode of interannual variability in the tropical Pacific climate system, significantly impacting global weather and climate. In the past several decades, extensive studies have led to substantial progress in understanding, modeling and predicting El Niño events (e.g., McCreary and Anderson, 1984; Cane and Zebiak, 1985; Zebiak and Cane, 1987; Philander, 1992; Wang et al., 2011, 2013). The delayed oscillator mechanism has been proposed to explain ENSO dynamics and its interannual oscillation within the tropical Pacific climate system (Battisti and Hirst, 1989). This theory emphasizes equatorial wave processes (Rossby wave and its reflection along the low-latitude western boundary into a Kelvin wave). Another is the recharge/discharge mechanism (Jin, 1997), which focuses on water exchange in the ocean on and off the Equator. As implied by these theories, the ENSO can be a cyclic oscillation between El Niño and La Niña conditions within the tropical Pacific climate system.

However, as observed, the ENSO also exhibits significant variability from one event instance to another. For example, multi-year cooling events can be seen during ENSO cycles from historical SST data (e.g., Hu et al., 2014). During 2010–12, the tropical Pacific had a persistent La Niña condition, with a second-year sea surface cooling that occurred in the fall of 2011. Further, many coupled models have failed to predict the Niño 3.4 sea surface temperature (SST) cooling when initialized from early- to mid-2011. Yet, one intermediate coupled model—an integrated climate model (ICM) operated at the Earth System Science Interdisciplinary Center (ESSIC), University of Maryland (UMD), the so-called ESSIC ICM (Zhang et al., 2003, 2005)—gave a successful forecast of the 2011 negative SSTAs with a lead time of one

* Corresponding author: FENG Licheng
Email: fenglich@nmefc.gov.cn

year or so (Zhang et al., 2013, 2014[a]). This presents a challenge to the ENSO prediction community and indicates an urgent need to understand processes leading to the second-year cooling.

Previously, ICM-based experiments were carried out to examine the roles played by the temperature of subsurface water entrained into the mixed layer, and wind forcing (Zhang et al., 2013, 2014[a]). The reappearance of a negative SSTA in the central equatorial Pacific in early summer of 2011 was closely related to off-equatorial thermal anomalies in the South Pacific. However, the three-dimensional structure and evolution of these have not been illustrated, as the oceanic processes responsible for the second-year cooling during the 2010–12 La Niña event are still poorly understood. The causes of the occurrence of a multi-year La Niña in general, and the 2011–12 La Niña event in particular, are not fully understood (Hu et al., 2014).

In this paper, we examine the oceanic processes responsible for the second-year cooling of the 2010–12 La Niña event using reanalysis data, with a focus on the roles played by off-equatorial subsurface anomalies in the South Pacific. To better represent pathways, isopycnal analyses were performed using three-dimensional temperature and salinity fields (Zhang and Rothstein, 2000). Since subsurface temperature anomalies tend to propagate along density surfaces, an isopycnal analysis can better characterize the three-dimensional structure and time evolution in a natural and physical way, therefore enabling us to trace pathways consistently throughout the basin. Our major finding was that a distinct pathway of off-equatorial temperature anomalies occurred along the South Equatorial Current (SEC), clearly associated with the onset of second-year cooling during the 2010–12 La Niña event. Through examining the subsurface temperature evolution on isopycnals, connections were more clearly illustrated between thermal anomalies at the subsurface and surface, and off and on the Equator, leading to an improved understanding of ENSO variability. Additionally, re-evaluating the historical ENSO evolution showed that another multi-year cooling case occurred in the tropical Pacific in 2007–09. The similarities and differences of these two events were analyzed to describe the nature of these strikingly different ENSO evolutions associated with various forcings and feedbacks within the Pacific climate system.

The remainder of the paper is organized as follows. We introduce the data and methodology used in this work in section 2. The results are presented in section 3, followed by a summary and discussion in section 4.

2. Data and methodology

Monthly-mean data for currents, sea surface height, temperature and salinity came from the Global Ocean Data Assimilation System (GODAS) (Behringer and Xue, 2004), operational at the National Centers for Environmental Prediction (NCEP). GODAS has a horizontal resolution of $1^\circ \times 1/3^\circ$ in the zonal and meridional directions; it has 40 levels in the vertical, with a 10 m resolution in the upper 200 m. We used the GODAS data covering the period from January 1980 through December 2012. Additionally, surface winds at 10 m height were from the NCEP–NCAR (National Center for Atmospheric Research) Reanalysis (Kalnay et al., 1996), with a longitudinal and latitudinal resolution of $1.904^\circ \times 1.875^\circ$ on a T62 Gaussian grid (192×94).

Long-term climatological fields were formed from the period 1980–2012, including monthly-mean current vectors. Interannual anomalies for temperature, wind stress and others were then calculated relative to their climatological fields. Finally, isopycnal surfaces were estimated using monthly temperature and salinity data. The temperature anomalies at level depths were interpolated to constant density surfaces by using a cubic spline. Climatological current vectors on isopycnal surfaces were formed in the same way. In this study, interannual anomaly fields on isopycnal surfaces were used to investigate the roles played by anomalous temperature advection in the 2010–12 and 2007–09 La Niña events.

3. Results

3.1. *SST evolution*

Figure 1 illustrates the horizontal distributions of SSTAs and surface wind anomalies for selected time intervals in 2011. In January, there was a La Niña state over the tropical Pacific. Consequently, negative SSTAs prevailed in the central and eastern tropical Pacific with the maxima exceeding -2°C between 150° and 170°W along the Equator. Surface easterly winds were stronger than normal over the western central equatorial Pacific and southeasterly wind anomalies dominated off the Equator in the South Pacific (Fig. 1a). Thereafter, the cold SSTA diminished and the SSTA became normal in the eastern tropical Pacific domain. Simultaneously, the wind stress anomalies weakened in most regions (Fig. 1b). This warming process persisted during the following months and peaked in June, when a neutral SST state prevailed throughout the Equator except for a weak negative anomaly along 160°W. At this time, easterly wind anomalies weakened in the central tropical Pacific (Fig. 1d). In August, negative SSTA strengthened in the central equatorial Pacific (Fig. 1f), and this cooling tendency persisted during the following months (Figs. 1g–h).

The mechanism of formation of the cold SSTA in the central eastern equatorial Pacific during mid–late 2011 has not been fully explained. Some possible factors, such as wind forcing or a subsurface thermal anomaly, may play an important role. Note that southeasterly wind became stronger in the tropical South Pacific (Fig. 1e), forcing the cold waters located in the South Pacific to move to the equatorial band (Fig. 1e) and leading to the negative SSTA. However, the cur-

[a]Zhang, R. -H, L. C. Feng, and Z. G. Wang, 2014: Role of atmospheric wind forcing in the second-year cooling of the 2010–12 La Niña event. *Atmos. Sci. Lett.*, submitted.

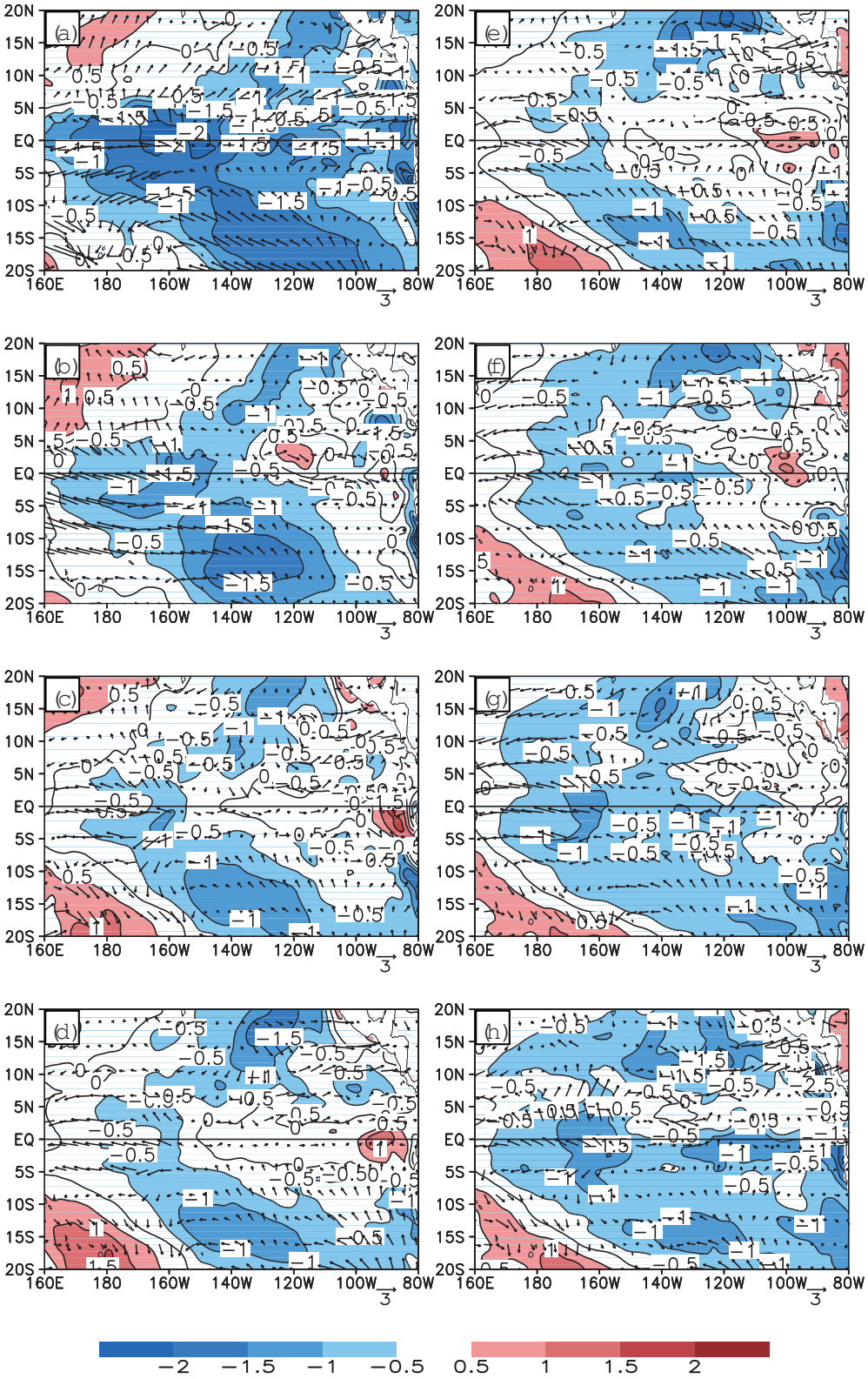

Fig. 1. Horizontal distributions of SSTA (at 5 m depth from GODAS) and wind anomalies during 2011 for (a) January, (b) March, (c) May, (d) June, (e) July, (f) August, (g) September, and (h) October. The contour interval is 0.5°C for SSTA, and the units for wind stress are dyn (1 dyn = 10^{-5} N) cm^{-2}.

rent driven by anomalous wind was not enough to produce strong and persistent negative SSTAs in the central equatorial Pacific, especially after the wind anomalies changed direction during September and October (Figs. 1g–h). Other

processes, such as subsurface effects, are required to fully understand the cause of the second-year cooling.

3.2. *Subsurface temperature anomaly pathway*

The climatological Bernoulli function (B) was calculated on the isopycnal surfaces to study the mean flow pattern. According to Cox and Bryan (1984), B can be written as

$$B(\sigma) = \rho_0 g\eta + g\int_{z(\sigma)}^{0} [\rho - \rho(\sigma)]dZ \ ,$$

where $\sigma = \rho - 1000$ is an isopycnal surface, and ρ is density with units of kg m^{-3}; ρ_0 is mean density; g is the acceleration due to gravity, and η is dynamic height. B represents geostrophic streamlines that measure the geostrophic flow away from the Equator; thus, it can be used to illustrate flow paths on isopycnal surfaces.

Figures 2a and 2c show the mean depth distributions of the 23.4 and 25.2 isopycnal surfaces. These two isopycnal surfaces had similar patterns in the tropical Pacific. On the Equator, the thermocline was deep in the west and shallow in the east. The deepest regions on the isopycnal surfaces were located around 15°N and 5°S, respectively, in the western central Pacific, with a relatively shallow band between 6° and 10°N. The isopycnal surfaces shoaled eastward along the Equator and reached minima in the far-eastern Pacific. The 23.4 isopycnal surface intersected with the sea surface (i.e., outcropped) in the central and eastern basin on and south of the Equator (Fig. 2a).

Pathways along which off-equatorial waters move onto the Equator have been examined in many studies (e.g. Zhang et al., 1999; Zhang and Busalacchi, 1999; Wang et al., 2007). However, most previous analyses focused on the effects in the North Pacific, with fewer studies in the South Pacific. Chang et al. (2001) pointed out the potential importance of south tropical Pacific variability in the decadal modulation of the ENSO. Luo et al. (2003) investigated the origin of the decadal ENSO-like variation. Luo et al. (2005) carried out 49-year simulations, and found that decadal variability of temperature and salinity along the Equator originates from subsurface spiciness anomalies in the South Pacific.

From Figs. 2b and d, one can see clear pathways originating from the southeastern tropical Pacific: water carried by the South Equator Current (SEC) extending northwestward to south of the equatorial band and then transported by the strong Equator Undercurrent (EUC) onto the Equator. The South Pacific water pathways intersect with the surface in the eastern equatorial and Southeast Pacific domain (Fig. 2b).

Figure 3 gives subsurface temperature anomalies evaluated on the 25.2 isopycnal surface (see Fig. 2c for its depth information) at some selected time periods in 2011; the vertical distribution of temperature anomalies in the upper ocean along the Equator is presented in Fig. 4. During the 2010–11 La Niña event, there was a buildup of warm waters in the western Pacific Ocean due to stronger than normal easterly winds in the central basin, characterized by positive thermal anomalies in the upper ocean. For example, in January 2011, a large positive anomaly was observed in the western central tropical Pacific and a negative anomaly was located

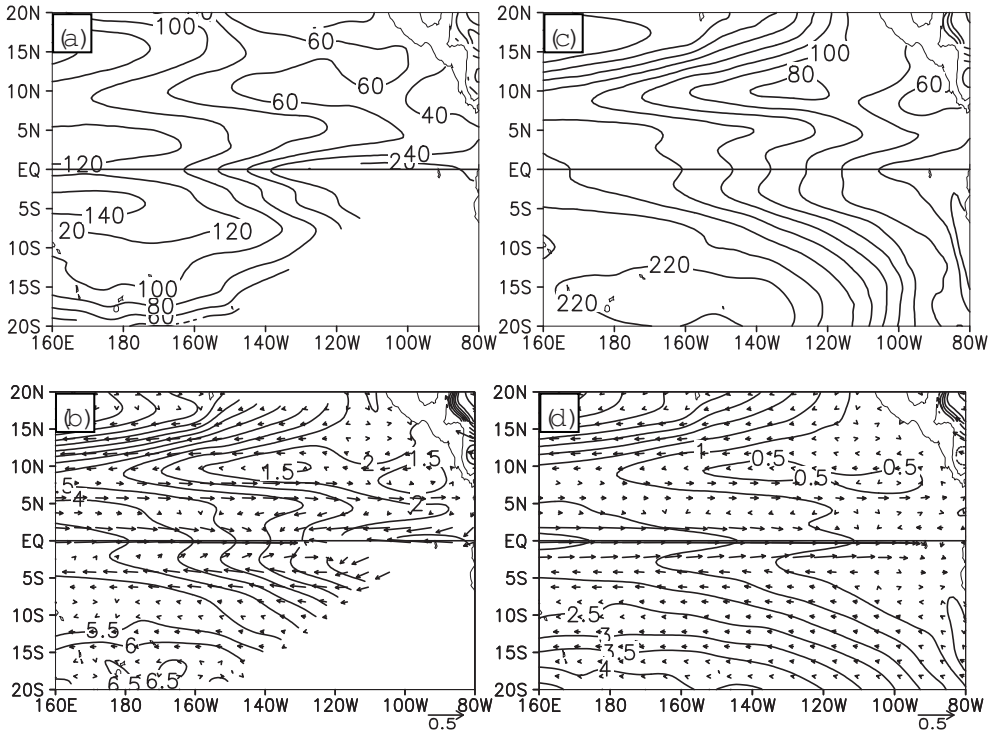

Fig. 2. Depths of the mean isopycnal surfaces, evaluated at (a) $\sigma = 23.4$ and (c) $\sigma = 25.2$. The Bernoulli function and current vectors calculated at (b) $\sigma = 23.4$ and (d) $\sigma = 25.2$. The contour interval is 20 m for the depth and 0.5 cm for the Bernoulli function.

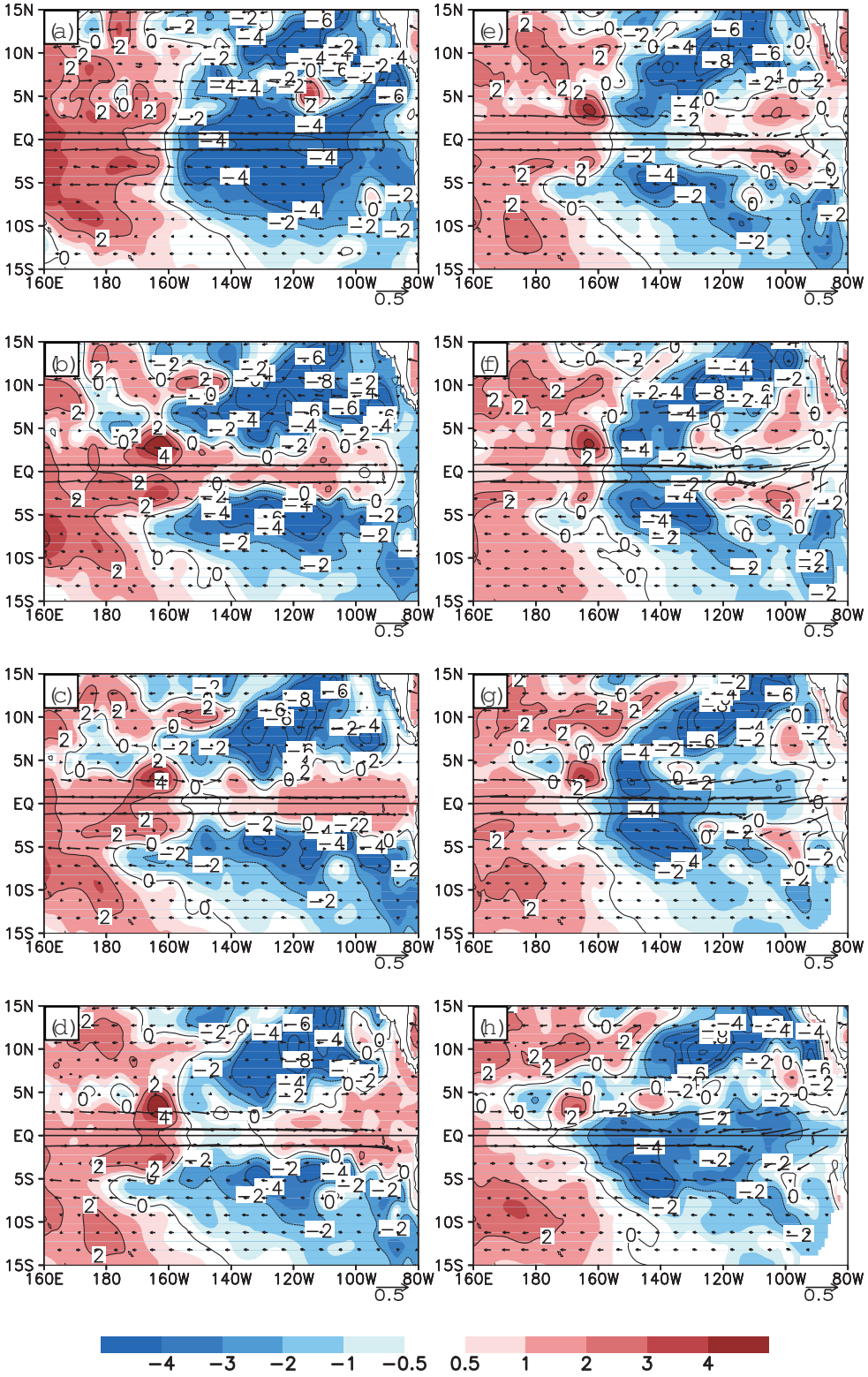

Fig. 3. Temperature anomalies evaluated on the $\sigma = 25.2$ isopycnal surface in 2011 for (a) January, (b) March, (c) April, (d) May, (e) June, (f) July, (g) August, and (h) September. The contour interval is 2°C. Superimposed are climatological current vectors for the corresponding months.

in the central eastern tropical Pacific regions. These two anomaly bands with opposite signs intersected along 160°W with a sharp temperature front (Figs. 3a and 4a). Beginning in early 2011, accompanied by the seasonal strengthening of the EUC, warm waters in the western Pacific expanded eastward across the Equator; cold anomalies in the central eastern equatorial Pacific diminished and reversed to above normal (Figs. 3b and 4b). This warming tendency peaked

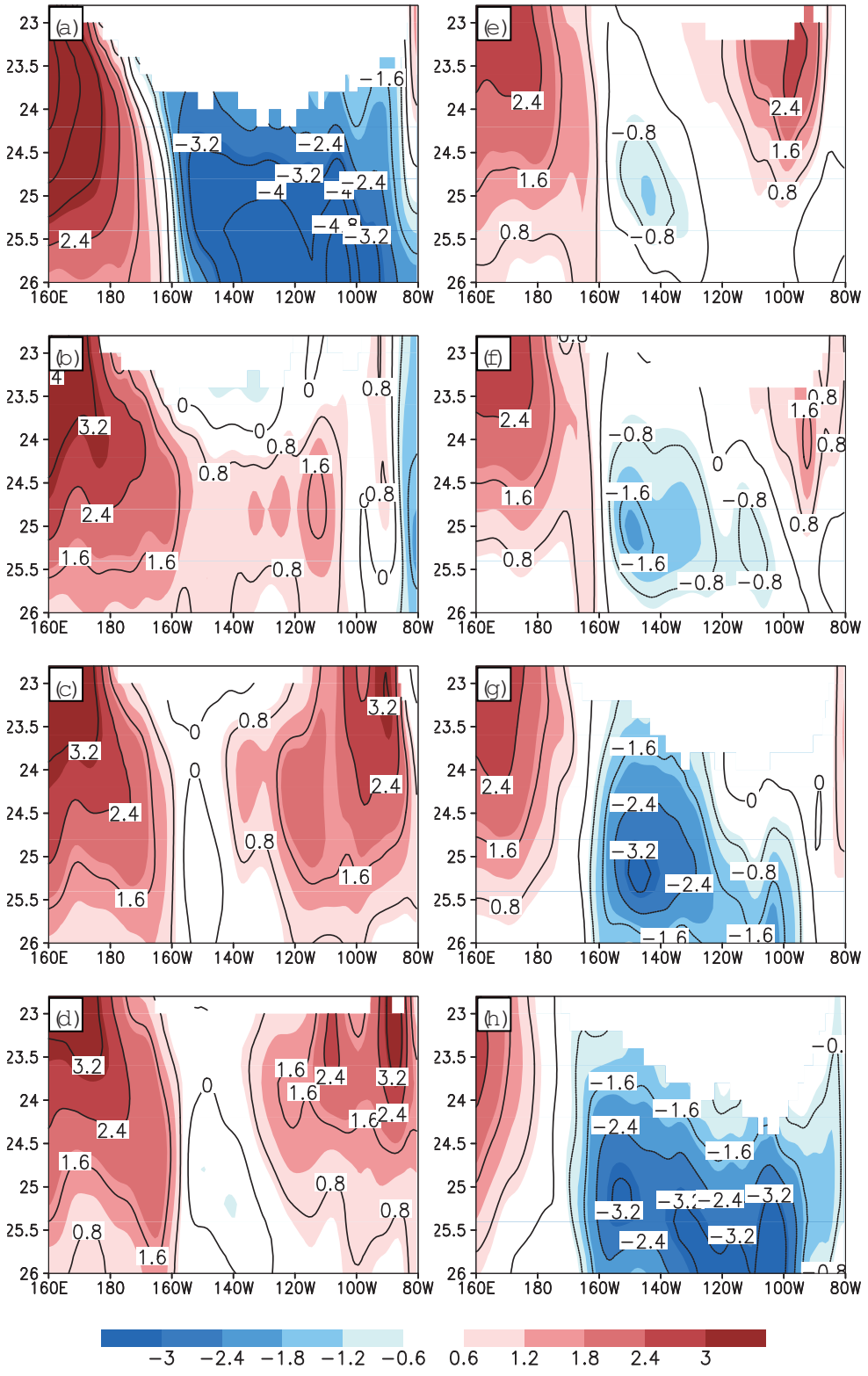

Fig. 4. Zonal sections of the upper ocean temperature anomalies along the Equator displayed on isopycnal surfaces as a vertical axis in 2011 for (a) January, (b) March, (c) April, (d) May, (e) June, (f) July, (g) August, and (h) September. The contour interval is 0.8°C.

in April (Fig. 3c), when positive temperature anomalies occupied almost the whole equatorial Pacific except for near 150°W. Temperature anomalies reached more than 2°C in the far-eastern equatorial Pacific. In the meantime, cold waters retreated to northeastern and southeastern regions off the Equator. As seen from the vertical section along the Equa-

tor (Fig. 4c), cold waters shrank back dramatically, and were confined to a narrow region of the central Pacific.

In May, positive anomalies along the Equator were seen to have two separate western and eastern bands (Fig. 3d), with below-normal temperature anomalies amplified in the regions of 140°–160°W (Fig. 4d). Subsequently, the neg-

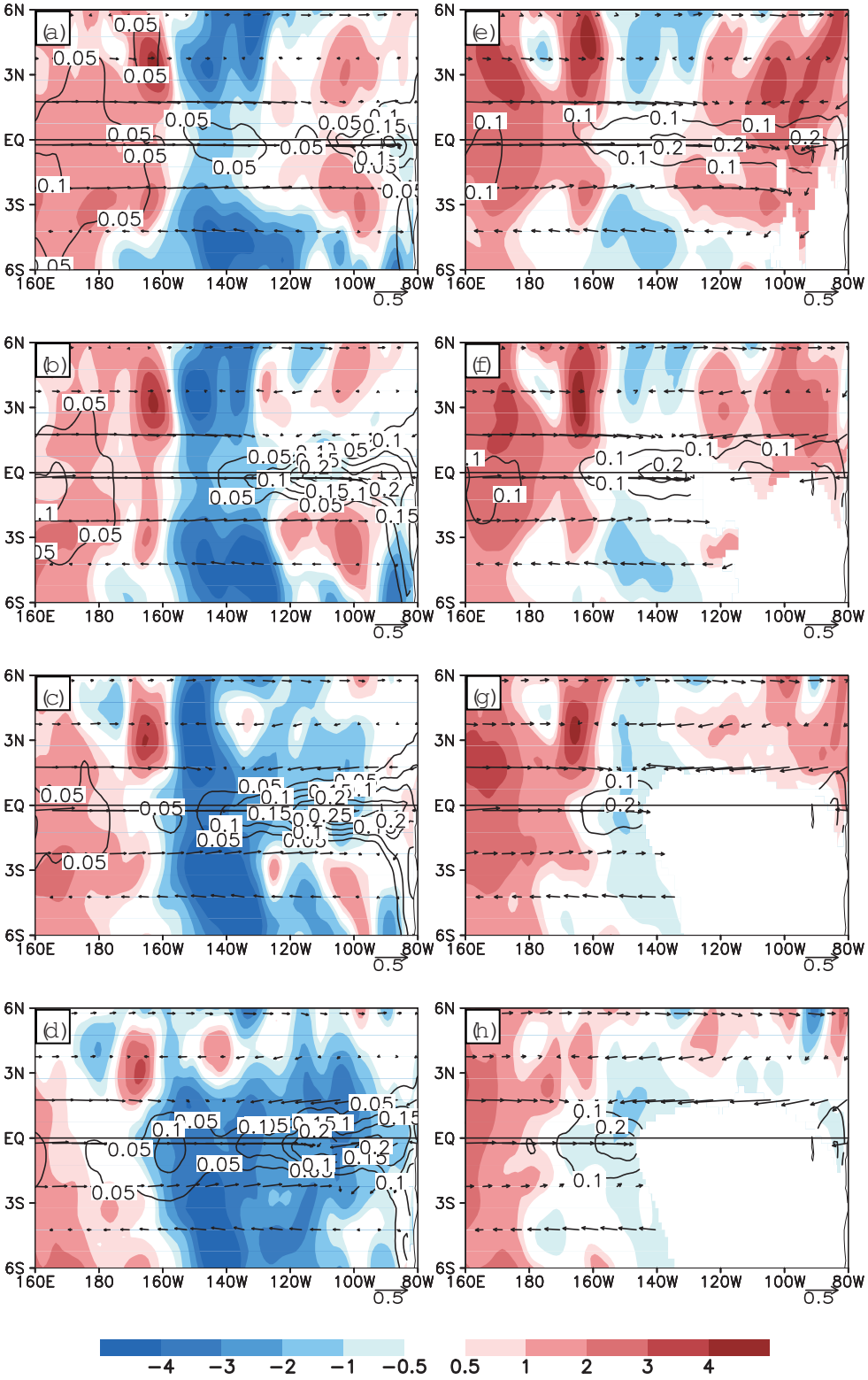

Fig. 5. Temperature anomalies evaluated on the $\sigma = 25.2$ (left) and $\sigma = 23.4$ (right) isopycnal surfaces in 2011 for (a, e) June, (b, f) July, (c, g) August, and (d, h) September. Superimposed are climatological current vectors and vertical velocity (contours) for the corresponding month.

ative anomalies dominated over the central Pacific in June (Fig. 3e), forming a horseshoe-like thermal anomaly pattern connecting large negative thermal anomalies on and off the Equator. Comparing Figs. 3e and 3d, the EUC decelerated in the far-eastern equatorial Pacific in June (Yu et al., 1997), but the off-equatorial cold anomalies strengthened in the central South Pacific. These changes were in favor of cold water advection to the equatorial regions through the well-defined South Pacific water pathway (Fig. 2d), and then extended into the equatorial region to combine with the negative anomalies located north of the Equator. In July, the EUC weakened further, and was even replaced by the SEC in the eastern Pacific on the 25.2 isopycnal surface. At this time, cold anomalies were transported by SEC from the Southeastern Pacific, and amplified on and off the central equatorial Pacific. This cooling tendency persisted in the following months. Positive anomalies along the Equator disappeared gradually, and cold anomalies dominated over the whole equatorial band (Figs. 3g and h). The vertical sections along the Equator displayed the same behavior (Figs. 4e–h).

3.3. *Phase relationships between subsurface and surface temperature anomalies*

As analyzed above, the subsurface thermal anomalies at the Equator exhibited similar evolution to the SSTAs, but with a 2 month phase lead time: negative sea temperature

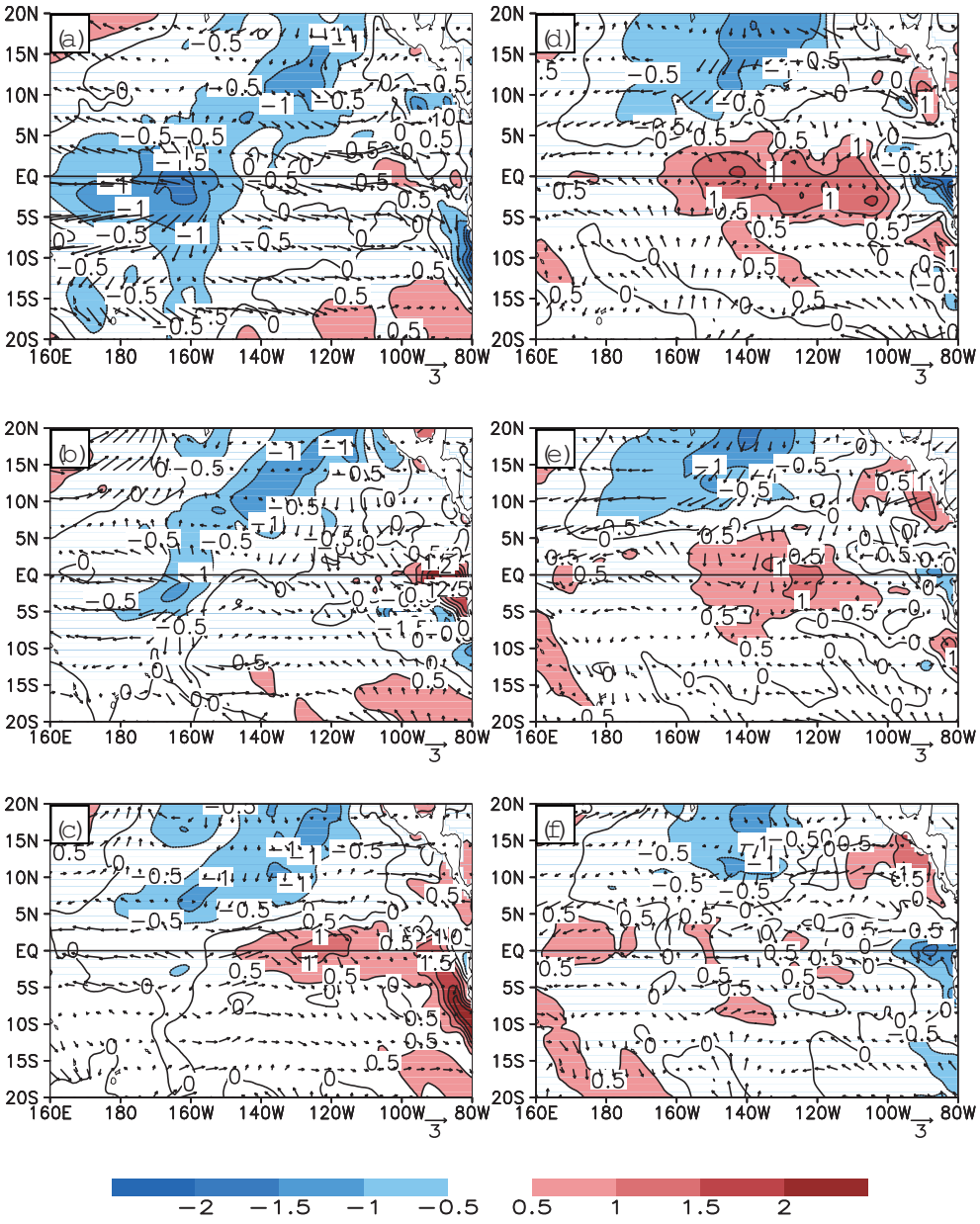

Fig. 6. Horizontal distributions of SSTA and wind anomalies during 2012 for (a) February, (b) April, (c) June, (d) August, (e) September, and (f) October. The contour interval is 0.5°C for SSTA, and the units for wind stress are dyn cm^{-2}.

anomalies (Fig. 3) re-strengthened at subsurface depths in June, while those in Fig. 1 re-strengthened at the sea surface in August. This indicates the existence of close links between subsurface temperature anomalies and the SSTAs. During boreal spring, positive SSTAs in the far-eastern equatorial Pacific (Figs. 1b and c) cannot be explained by surface temperature advection, and they are likely to originate from the outcrop of subsurface warm anomalies (Figs. 4b and c). This process can be described as follows. During the previous La Niña event, warm waters piled up in the western Pacific Ocean due to stronger than normal easterly winds in the central basin. As the EUC became seasonally strengthened, the subsurface warm water was transported from the western Pacific to the central and eastern Pacific across the Equator (Figs. 3b–c). Since the thermocline shoaled eastward (Figs. 2a and c), the warm water was exposed to the sea surface in the eastern Pacific, acting to generate positive SSTAs (Figs. 1b and c; Figs. 4b and c).

As for the sea surface cooling in the fall of 2011, it can be traced to the subsurface anomalies. Beginning in mid-2011, subsurface cold anomalies located in the southeastern tropical Pacific were continually advected northwestward by the SEC, to the south of the equatorial band, and then transported by the EUC to the Equator, where they were accumulated (Figs. 3e–h). But how did the subsurface cold water in the central Pacific affect the sea surface? Since there was no systematic surface wind stress curl (figures not shown), the related Ekman pumping was not a major factor influencing the outcropping of subsurface cold water, so the upwelling can only be driven by oceanic processes. Figure 5 presents the tempera-

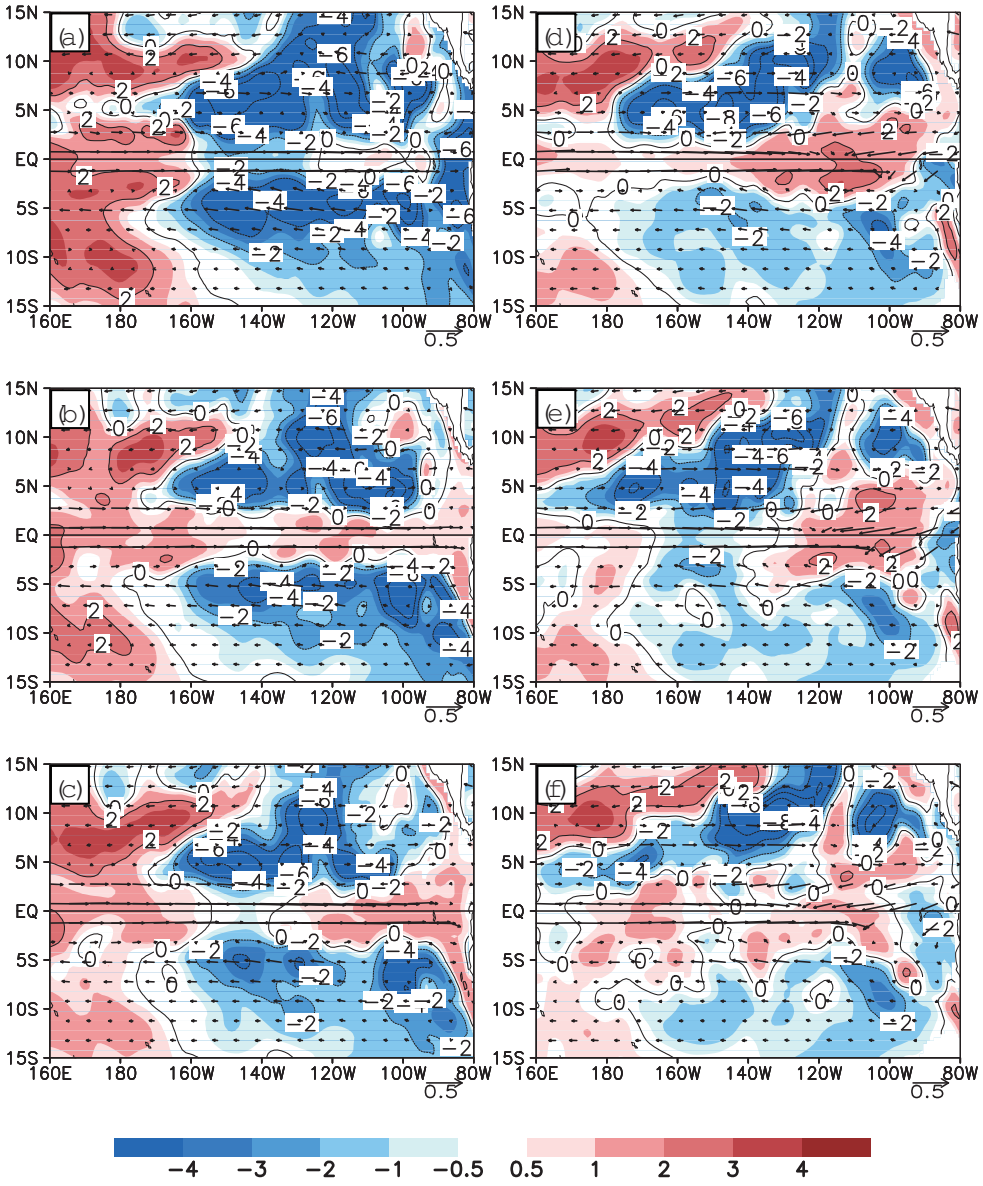

Fig. 7. Temperature anomalies evaluated on the $\sigma = 25.2$ isopycnal surface in 2012 for (a) March, (b) May, (c) June, (d) August, (e) September, and (f) October. The contour interval is 2°C. Superimposed are climatological current vectors for the corresponding month.

ture anomalies, and the horizontal and vertical velocity fields on the 23.4 and 25.2 isopycnals. The convergence pattern of the horizontal currents agreed reasonably well with the vertical velocity field. For example, the convergence center was located on the Equator near 110°W, where the EUC met the SEC, giving rise to a strong upwelling (Fig. 5b).

In June, small cold anomalies were accompanied by weak upwelling in the central equatorial Pacific (Fig. 5a). With time, both cold anomalies and vertical velocity strengthened in the central equatorial Pacific on the 25.2 isopycnal surface (Figs. 5b and c). For example, in June the cold anomalies were confined between 130°W and 150°W along the Equator, but it dominated the eastern central Pacific in July. These changes were induced by the weakened EUC and strengthened SEC, which favored the accumulation of cold water at the Equator. Figures 5e–h indicate that the vertical current in the upper layer was stronger than that at the lower layer (Figs. 5a–d), and the cold anomalies appeared later than that on the subsurface layer, which confirmed that the cold water originated from the subsurface. As discussed above, there was a clear pathway along which subsurface cold water was transported to the sea surface. Firstly, the subsurface cold water located in the southeastern tropical Pacific was advected by the SEC south of the Equator. Subsequently, the EUC transported it to the equatorial Pacific, where the EUC met the SEC and induced upwelling. Finally, under the effects of the EUC and SEC, the cold water spread upward and westward to the sea surface.

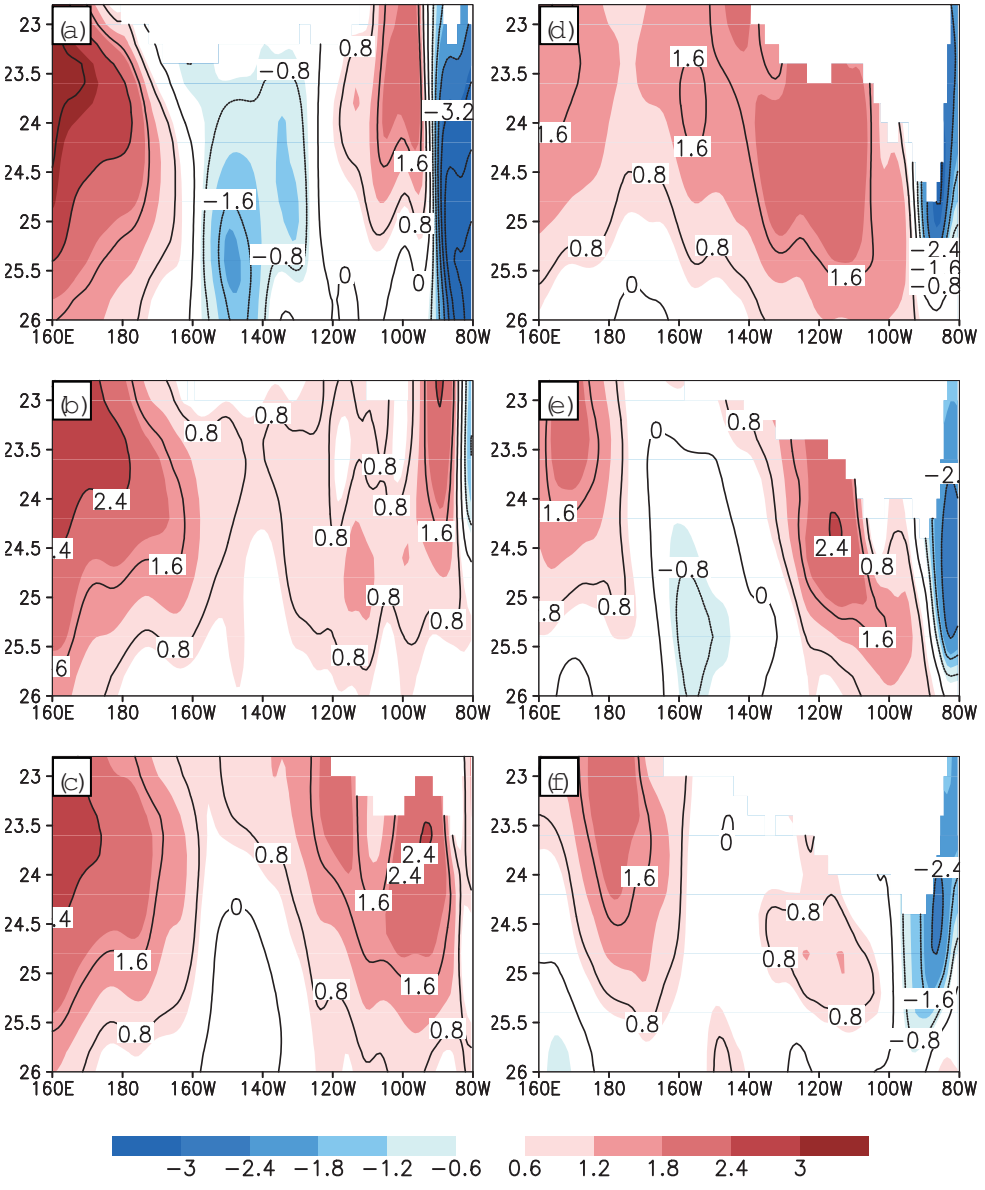

Fig. 8. Zonal sections of the upper ocean temperature anomalies along the Equator displayed on isopycnal surfaces as a vertical axis in 2012 for (a) March, (b) May, (c) June, (d) August, (e) September, and (f) October. The contour interval is 0.8°C.

In the fall of 2011 (Figs. 1g and h), negative SSTAs dominated in the central and eastern equatorial Pacific basin. The negative SSTAs in the east affected winds to the west, which in turn affected the thermocline and SST in the east. This essentially involved interactions among anomalies of SST, wind and the thermocline, forming a coupling loop and leading to the second-year cooling during 2010–12.

3.4. *Evolution during the 2012 decay phase*

Figure 6 gives the horizontal distributions of SSTAs and surface wind anomalies at some selected time intervals in 2012. From February onwards, the cold SSTA diminished and the SSTA became normal in the eastern tropical Pacific domain (Fig. 6a). This warming process persisted during the following months, and the SSTAs in the central and eastern tropical Pacific rose above normal (Fig. 6d), except in the far-eastern Pacific. Figure 7 illustrates the subsurface temperature anomalies evaluated on the 25.2 isopycnal surface at some selected time periods in 2012; the vertical distribution of temperature anomalies in the upper ocean along the Equator is presented in Fig. 8. Beginning in early 2012, accompanied by the seasonal strengthening of the EUC, warm waters in the western Pacific expanded eastward across the Equator (Figs. 7a and 8a). In May, with the seasonal maximum EUC, warm anomalies occupied the whole central eastern equatorial Pacific (Figs. 7b and 8b). Negative anomalies re-emerged twice (Figs. 7c and e; Figs. 8c and e) in the central equatorial Pacific, since the EUC decelerated from June onwards. However, these cooling processes did not persist and develop, perhaps because the cold anomalies in the South Pacific were

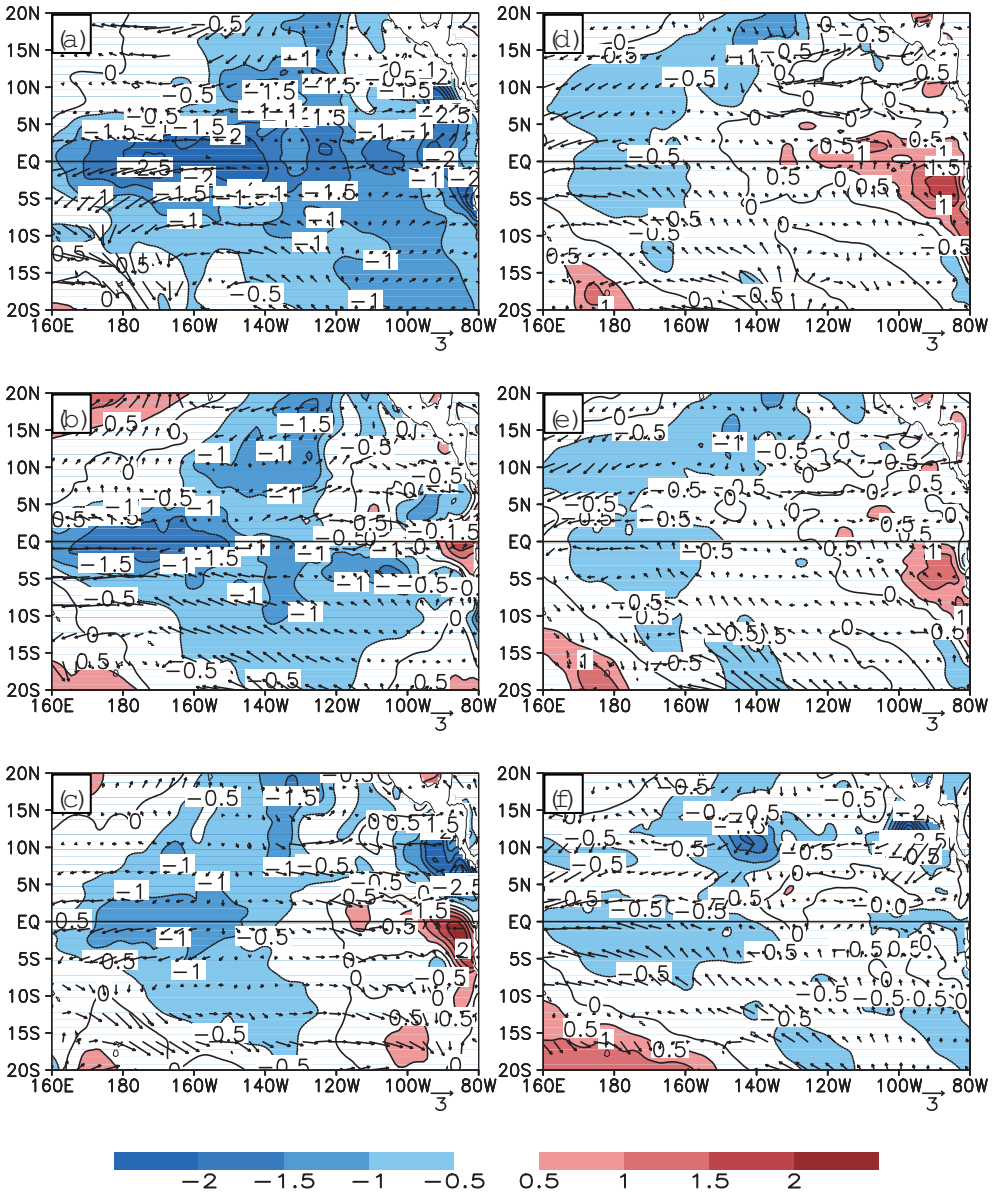

Fig. 9. Horizontal distributions of SSTA and wind anomalies during 2008 for (a) January, (b) March, (c) May, (d) August, (e) September, and (f) November. The contour interval is 0.5°C for SSTA, and the units for wind stress are dyn cm^{-2} (1 dyn = 10^{-5} N).

too weak to provide enough cold water (Figs. 7d–f; Figs. 8d–f). Finally, the SSTAs did not return to the La Niña state, as happened during 2011.

3.5. *Evolution during the 2008 La Niña event*

Figure 9 gives the horizontal distributions of the SSTAs and surface wind anomalies at some selected time intervals

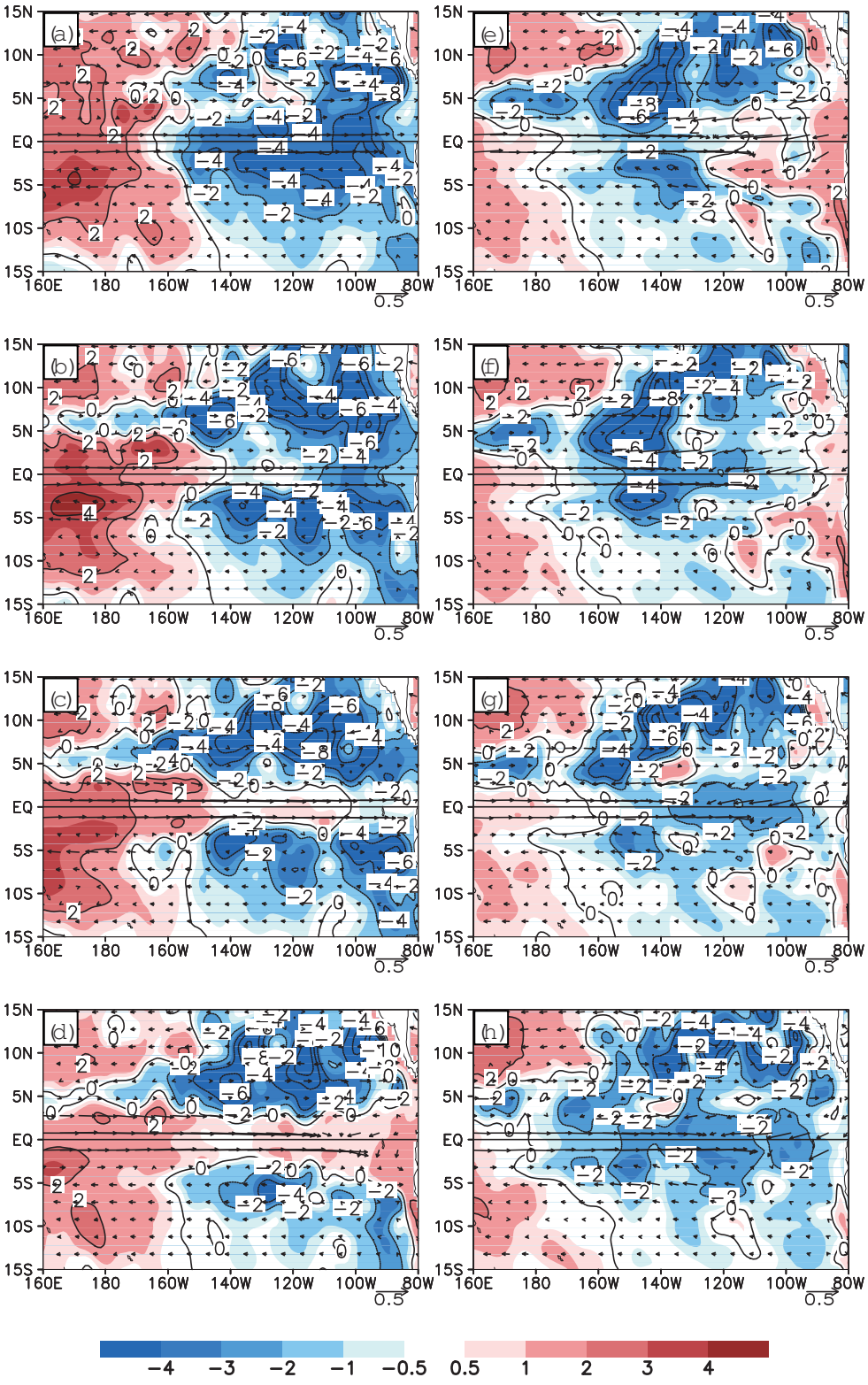

Fig. 10. Temperature anomalies evaluated on the $\sigma = 25.4$ isopycnal surface in 2008 for (a) January, (b) March, (c) April, (d) June, (e) August, (f) September, (g) October, and (h) November. The contour interval is 2°C. Superimposed are the climatological current vectors for the corresponding month.

in 2008. In January, a La Niña state occupied the tropical Pacific: negative SSTAs prevailed in the central and eastern tropical Pacific with the maxima exceeding −2.5°C, located at 170°W along the Equator (Fig. 9a). Thereafter, the cold SSTA diminished and the SSTA increased above normal in the far-eastern tropical Pacific domain (Fig. 9b). This warm-

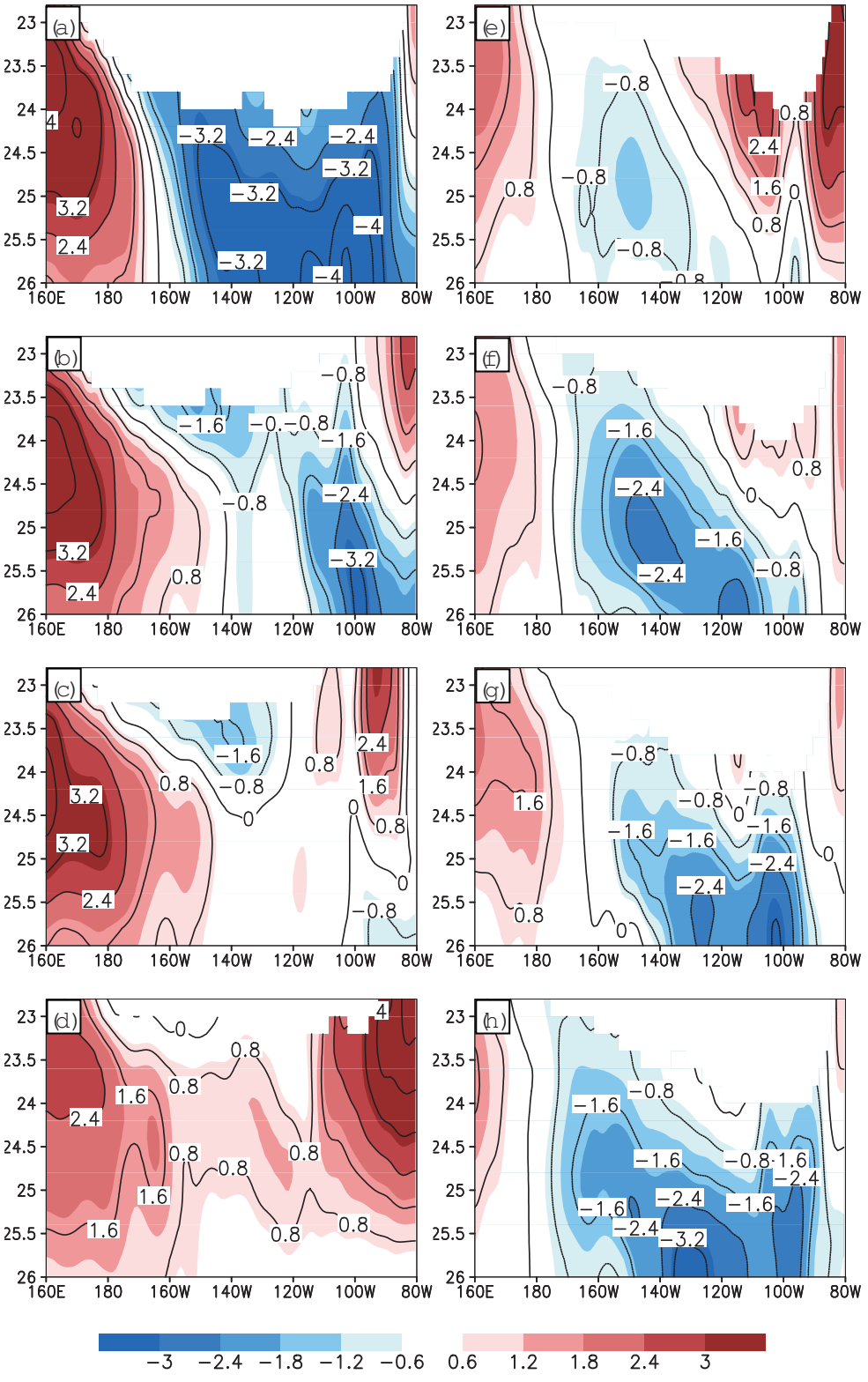

Fig. 11. Zonal sections of the upper ocean temperature anomalies along the Equator displayed on isopycnal surfaces as a vertical axis in 2008 for (a) January, (b) March, (c) April, (d) June, (e) August, (f) September, (g) October, and (h) November. The contour interval is 0.8°C.

ing process persisted during the following months and peaked in August (Fig. 9d). In September, the negative SSTA re-strengthened in the central equatorial Pacific (Fig. 9e), and this cooling tendency persisted during the following months (Fig. 9f).

Figure 10 illustrates the subsurface temperature anomalies evaluated on the 25.4 isopycnal surface at some selected time periods in 2008; the vertical distribution of temperature anomalies in the upper ocean along the Equator is presented in Fig. 11. Beginning in early 2008, accompanied by the seasonal strengthening of the EUC, warm waters in the western Pacific expanded eastward across the Equator (Fig. 10b). This warming tendency peaked in mid-2008 (Figs. 10d and 11d), when positive temperature anomalies occupied almost the whole equatorial Pacific. There was a 1–2 month lead time into the SSTAs. Compared with the warming process in 2011 (Figs. 3c and 4c), it lagged by about 2 months, possibly attributable to stronger negative anomalies in the eastern tropical Pacific. Beginning in August, the subsurface cold anomalies located in the southeastern tropical Pacific were continually advected northwestward by the SEC to the south of the equatorial band, and then transported by the EUC to the Equator, where they accumulated (Figs. 10e–h). The cold anomalies were then transported by a vertical current to the sea surface and induced negative SSTAs. From September, cold water re-strengthened in the central-equatorial Pacific (Fig. 9e), and this cooling tendency persisted and extended eastward during the following months (Figs. 9h); consequently, the double-trough La Niña developed.

4. Summary and discussion

The reanalysis products from GODAS were used to produce isopycnal surfaces to better illustrate and understand the processes leading to the second-year cooling of the 2010–12 La Niña event. We found anomaly patterns originating at depth from the southeastern tropical Pacific that could be responsible for generating and sustaining negative SSTAs in the central equatorial Pacific.

A sequence of events leading to the La Niña conditions in the fall of 2011 was described. During the 2010 La Niña event, warm waters piled up at subsurface depths in the western tropical Pacific. Beginning in early 2011, and accompanied by a strong EUC, subsurface warm waters in the western Pacific transmitted eastward along the Equator. Positive temperature anomalies occupied the equatorial Pacific in April, and cold waters retreated to northeastern and southeastern off-equatorial Pacific regions. Since the thermocline shoaled along the Equator and was close to the surface in the eastern Pacific, subsurface warm waters were directly exposed to the sea surface in the eastern Pacific, and induced a warm SSTA. Normal SST conditions appeared in the central and eastern equatorial Pacific in mid-2011.

In August a negative SSTA reappeared in the central Pacific. We hypothesized that this anomaly came from the subsurface cold waters off the Equator through the Southern Pacific pathway. Based on the GODAS analyses, the processes were described as follows: Cold anomalies located in southeastern tropical Pacific region were advected continually by the SEC northwestward to the south of the equatorial band, and then by the EUC northeastward to the Equator. With time, the EUC weakened and the SEC strengthened in the eastern equatorial Pacific, inducing cold waters that accumulated in the central tropical Pacific and then tended to spread upward with the convergence of horizontal currents and eventually outcropped to the surface. These subsurface-induced SSTAs acted to initiate local coupled air–sea interactions generating atmospheric–oceanic anomalies that developed and evolved with the second-year cooling in the fall of 2011.

Further study of the 2012 processes indicated that the cooling tendency did not develop into another La Niña event, since the cold anomalies in the South Pacific were not strong enough. An analysis around the 2007–09 La Niña event revealed similar evolution processes with around a 2—month phase lag, compared to the 2010–12 La Niña event.

These analyses provide an observational basis for an understanding of the processes involved. The results can be used to explain the ways in which coupled models predict the second-year cooling case, and offer guidance for historical analyses for other multi-year cooling events. Further supporting modeling studies are needed to quantify the role played by off-equatorial subsurface anomalies in triggering La Niña events in the tropical Pacific. Here, we discussed the effect of interannual variability on the multi-year cooling. The effect of modulation of decadal to interdecadal timescale variability on the multi-year cooling, such as tropical Pacific decadal variability (Choi et al., 2013), requires further study.

Acknowledgements. This work has benefited a great deal from Prof. A. J. BUSALACCHI's support. This research was jointly supported by National Natural Science Foundation of China (Grant No. 40906014), the Ocean Public Welfare Scientific Research Project (Grant No. 201205018-2), the National Key Basic Research Program of China (Grant No. 2010CB950302), and the China Scholarship Council (CSC). ZHANG is supported partly by the National Science Foundation (NSF) (Grant No. ATM-0727668), NASA (Grant No. NNX08AI74G), and the National Oceanic and Atmospheric Administration (NOAA) (Grant No. NA08OAR4310885).

REFERENCES

Battisti, D. S., and A. C. Hirst, 1989: Interannual variability in the tropical atmosphere-ocean system: Influence of the basis state, ocean geometry and nonlinearity. *J. Atmos. Sci.*, **46**, 1687–1712.

Behringer, D. W., and Y. Xue, 2004: Evaluation of the global ocean data assimilation system at NCEP: The Pacific Ocean. Preprints, *Eighth Symp. on Integrated Observing and Assimilation Systems for Atmosphere, Oceans, and Land Surface*, Seattle, WA, Amer. Meteor. Soc., 2. 3. [Available online at https://ams.confex.com/ams/84Annual/techprogram/paper_70720.htm.]

Cane, M. A., and S. E. Zebiak, 1985: A theory for El Niño and the Southern Oscillation. *Science*, **228**, 1085–1087.

Chang, P., B. S. Giese, L. Ji, H. F. Seidel, and F. Wang, 2001: Decadal change in the South Tropical Pacific in a global assimilation analysis. *Geophys. Res. Lett.*, **28**, 3461–3464.

Choi, J., S. I. An., S. W. Yeh, and J. Y. Yu, 2013: ENSO-like and ENSO-induced tropical Pacific decadal variability in CGCMs. *J. Climate*, **26**, 1485–1501.

Cox, M. D., and K. Bryan, 1984: A numerical model of the ventilated thermocline, *J. Phys. Oceanogr.*, **14**, 674–687.

Hu, Z. -Z., A. Kumar, Y. Xue, and B. Jha, 2014: Why were some La Niña followed by another La Niña? *Climate Dyn.*, **42**, 1029–1042, doi: 10.1007/s00382-013-1917-3.

Jin, F. -F., 1997: An equatorial ocean recharge paradigm for ENSO. Part I: Conceptual model. *J. Atmos. Sci.*, **54**, 811–829.

Kalnay, E., and Coauthors, 1996: The NCEP/NCAR 40-year reanalysis project. *Bull. Amer. Meteor. Soc.*, **77** (3), 437–471.

Luo, J.-J., S. Masson, S. K. Behera, P. Delecluse, S. Gualdi, A. Navarra, and T. Yamagata, 2003: South Pacific Origin of the decadal ENSO-like variation as simulated by a coupled GCM. *Geophys. Res. Lett.*, **30**(24), 2250, doi: 10.1029/2003GL018649.

Luo, Y. -Y., L. M. Rothstein, R.-H. Zhang, and A. J. Busalacchi, 2005: On the connection between South Pacific subtropical spiciness anomalies and decadal equatorial variability in an ocean general circulation model. *J. Geophys. Res.*, **110**, C10002, doi: 10.1029/2004JC002655.

McCreary, J. P. Jr., and D. L. T. Anderson, 1984: A simple model of El Niño and the Southern Oscillation. *Mon. Wea. Rev.*, **112**, 934–946.

Philander, S. G. H, 1992: Ocean-atmosphere interactions in the tropics: A review of recent theories and models. *J. Appl. Meteoro.*, **31**, 938–945.

Wang, X., C. Y. Li, and W. Zhou, 2007: Interdecadal mode and its propagating characteristics of SSTA in the South Pacific. *Meteor. Atmos. Phys.*, **98**, 115–124, doi: 10.1007/s00703-006-0235-2.

Wang, X., C. Z. Wang, W. Zhou, D. X. Wang, and J. Song, 2011: Teleconnected influence of North Atlantic sea surface temperature on the El Niño onset. *Climate Dyn.*, **37**, 663–676, doi: 10.1007/s00382-010-0833-z.

Wang, X., C. Z. Wang, W. Zhou, L. Liu, and D. X. Wang, 2013: Remote influence of North Atlantic SST on the equatorial westerly wind anomalies in the western Pacific for initiating an El Niño event: An Atmospheric General Circulation Model Study. *Atmos. Sci. Lett.*, **14**, 107–111.

Yu, Z.-J., P. S. Schopf, and J. P. McCreary Jr., 1997: On the annual cycle of upper-ocean circulation in the eastern equatorial Pacific. *J. Phys. Oceanogr.*, **27** 309–324.

Zebiak, S. E., and M. A. Cane, 1987: A model El Niño-Southern Oscillation. *Mon. Wea. Rev.*, **115**, 2262–2278.

Zhang, R.-H., and A. J. Busalacchi, 1999: A possible link between off-equatorial warm anomalies propagating along the NECC path and the onset of the 1997–98 El Niño. *Geophys. Res. Lett.*, **26**(18), 2873–2876.

Zhang, R. -H., and L. M. Rothstein, 2000: Role of off-equatorial subsurface anomalies in initiating the 1991-1992 El Niño as revealed by the National Centers for Environmental Prediction ocean reanalysis data. *J. Geophys. Res.*, **105**(C3), 6327–6339.

Zhang, R.-H., L. M. Rothstein, A. J. Busalacchi, and X. Z. Liang, 1999: The onset of the 1991-92 El Niño event in the tropical Pacific Ocean: The NECC subsurface pathway. *Geophys. Res. Lett.*, **26**(7), 847–850.

Zhang, R.-H., S. E. Zebiak, R. Kleeman, and N. Keenlyside, 2003: A new intermediate coupled model for El Niño simulation and prediction. *Geophys. Res. Lett.*, **30**(19), doi: 10.1029/2003GL018010.

Zhang, R. -H., S. E. Zebiak, R. Kleeman, and N. Keenlyside, 2005: Retrospective El Nino forecast using an improved intermediate coupled model. *Mon. Wea. Rev.*, **133**, 2777–2802.

Zhang, R. -H., F. Zheng, J. Zhu, and Z. G. Wang, 2013: A successful real–time forecast of the 2010–11 La Niña event. *Sci. Rep.*, **3**, 1108, doi: 10.1038/srep01108.